Analysis of the Optical Performances of the Solar Tower Power Plant

M. Bouamra*[1], M. Merzouk[1]

[1]FundApl

[1]Saad Dahlab University, Street of Soumaa, Blida ,Algeria

*bouamram@gmail.com

Abstract— The central receiver system (CRS) concept is an attractive method to achieve an extremely high concentration of solar radiation for electrical power generation, and other applications, on a large-scale. In this paper we present an algorithm giving the preliminary design of a solar field of heliostats in a solar tower power plant in order to define the optimal position coordinates to each heliostat. From this position we can analyze the optical performance of the plant in a preliminary manner for any point design given. The results obtained by this method of programming for optimization of a circular field of heliostats are in good concordance with those found in the literature, both in the geometric distribution of the solar field, and value of the optical efficiency. We have continued this work to study the distribution of solar flux on the receiver, reflected by each of heliostat. The model is applied to a group of heliostats of a real field to obtain the resulting flux distribution.

Keywords- field; optical; heliostat; efficiency; program; attenuation.

I. INTRODUCTION

The central receiver system (CRS), also known as Tower Solar Power, is a concentrating solar power technology consisting of a heliostat field where each heliostat tracks the sunrays by means of a two-axes system and concentrates them on a solar receiver located at the top of a tower [1](Fig 1). The concentrated energy is absorbed efficiently by a fluid circulating within the receiver. The heat transfer fluid (HTF) is circulated through the receiver to absorb radiation heat and transport it either to the hot tank thermal energy storage (TES) or directly to the power cycle and steam heating heat exchanger. Solar tower technology is capable of providing high temperature up to 2200 k [2], can be used directly or indirectly to drive a turbine to produce electrical energy, as process heat in industrial applications, or to produce hydrogen [3]. Expected that the direction of the solar rays are not parallel (an observer on Earth sees the sun at an angle of 32 ') and otherwise the heliostats used by power towers are plans. The result is a no uniform distribution of the radiant flux density at the sunspot, which is a surface necessarily occupied by a boiler. Thus, we will have at the receiver a surface instead of a point with maximum power at the center and a ring less dense. The purpose of this work is to define and study the position coordinates for each of heliostats that form the solar field, to determine the best position. From this position we can evaluate the optical efficiency, compare the model results with the literature and then examine the density distribution of the solar flux on the receiver, reflected by each of the heliostats.
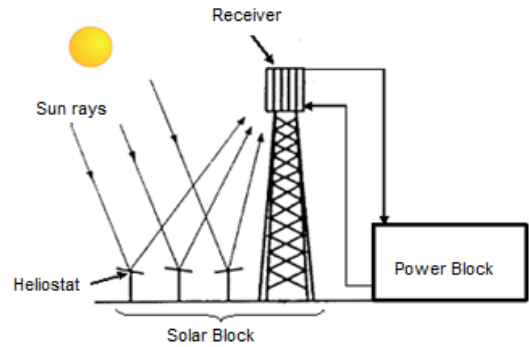

Fig.1 Schematic representation of tower solar power.

II. OPTIMIZATION OF HELIOSTAT FIELD AND AVERAGE OPTICAL ENFFICIECY

A. Optimization of heliostat field

The performance of the heliostat field is defined in terms of the optical efficiency, defined as a ratio of the net power intercepted by the receiver to the power incident normally on the field. The optical losses include the cosine effect, shading and blocking losses, imperfect mirror reflectivity, atmospheric attenuation, and receiver spillage losses. Clearly, the heliostats should be carefully distributed in the field, so that maximum efficiency is obtained [4]. The preliminary design of the proposed heliostat field is based on the full radial staggered configuration of the heliostats from the center of the base of the tower. The radius of the first row is defined as 0.5 Ht [5], where Ht is the tower optical height. The radial distance ΔR between consecutive rows keeping the blocking factor constant through the heliostat field is defined as[5,6].

$$\Delta R = \left[\left(\frac{cos\ \omega}{cos\ \varepsilon_T} \right) \left(1 - \frac{(1-f_b)wr}{2wr - \left(\sqrt{1+wr^2}+ds\right)} \right) \right] LH \qquad (1)$$

Where f_b is the blocking factor, wr is the width-height ration of the heliostat, LH is the height of the heliostat, ω is the incidence angle of the sunrays onto the heliostat surface, ε_T is the elevation angle of the tower unit vector pointing from the center of heliostat surface to the receiver and $ds.LH$ is any additional security distance between adjacent heliostats in the same row.

B. Average optical efficiency of heliostat field

The local optical efficiency of each heliostat is given by [5,7,8]:

$$\eta_f = \rho.\cos\omega_i.f_b.f_{sp}.f_{at} \qquad (2)$$

Where ω_i is the incidence angle, is calculated using the law of specular reflection. The dot product of unitary sun vector (pointing towards the sun) and the unit normal to the heliostat surface give us the cosine efficiency [9].

$$\cos\omega_i = \overrightarrow{d_{sun}}.\overrightarrow{d_n} \qquad (3)$$

ρ is the reflectivity of the mirrors and f_{sp} is the spillage factor were both assumed equal to 1, f_b is blocking factor, in this formula the shadows are neglected and f_{at} is atmospheric attenuation factor. For a clear day is [10] :

$$f_{at} = 0,99326 - 0,1046.d + 0,0017.d^2 - 0,002845.d^3 \quad (4)$$

Where d is the slant range from heliostat to receiver in kilometers. The atmospheric attenuation for a hazy day is [4]:

$$f_{at} = 0,98707 - 0,2748.d + 0,03394.d^2 \qquad (5)$$

The average optical efficiency of heliostat field is given by [11]:

$$\eta_{f_{solar\ field}} = \frac{\sum_{i=1}^{i=heliostats} \eta_{f_i}}{number\ of\ heliostats} \qquad (6)$$

III. MODELING FLUX ON THE RECEIVER

Our study is based on a vertical receiver for arrangement of heliostats north to the tower. Different methods exist [12] for the simulation of the flux distribution produced by heliostats. Existing models are divided into two categories [13]: Monte Carlo Ray Tracing (MCRT) and convolution methods. The first one is a statistical approach that traces a bundle of random rays from the sun. The more rays are traced the higher precision is achieved, but also higher computational cost, unaffordable for design and optimization studies. On the other hand, convolution methods rely on the mathematical superposition of error cones, namely: sunshape, concentration and mirror errors. While several approaches have been proposed to solve the convolution integral, all of them are faster than MCRT techniques. In this work we utilize the method proposed by Collado et al. [14], due to its clear advantage in computational speed. The used method is based on assuming continuous heliostat facets of spherical curvature, circular effective sun shape and conformal mapping between the heliostat plane and the image of aperture receiver plane. And we assume for the purposes of simplifying the size of the problem, the distance between any point taken from the surface of the heliostat and the center of the receiver is identical to the distance between the center of the heliostat and the center of the receiver. In this case the mathematical expression for the flux density sent by heliostat on the receiving plane can be expressed as [14]:

$$F(x_r, y_r) = \frac{C_r.I_d.\rho.f_{at}.(AM/AH)}{4} \cdot \{erf(\xi_r + a_{1r}) - erf(\xi_r - a_{1r})\} \cdot \\ \{erf(\zeta_r + a_{2r}) - erf(\zeta_r - a_{2r})\} \qquad (7)$$

Where :AM is total area of the heliostat mirrors, AH is the surface of the heliostat ,Cr is the concentration function due to the reflection law on the receiver plane, a_{1r} et a_{2r} are dimensions of the heliostat transformed on the receiver , I_d direct solar irradiation and erf is the error function . To find the variables ξ_r and ζ_r corresponding to the coordinates of the heliostat transformed on the receiver plane, it is convenient to subdivide the surface of the heliostat in mesh, after from each point taken on the plan of the heliostat we can find its image through the transition matrices on the receiver plane and hence obtain the flux distribution reflected by each heliostat.

IV. RESULTS AND DISCUSSIONS

A. Validation:

To check our program for generating preliminary heliostat fields, data have been used of some basic field parameters based on [5]. Figures 2 and 3, allow us to compare the field efficiency of Collado 2009[5] with our work, for a circular field of 17 lines, a blocking factor = 0.95 and the point of design is Spring equinox. To observe graphically the distribution of the field efficiency on the field, the heliostats circles were colored according to their efficiency levels.

1) General dimensions of the heliostat field: Regarding Collado model, it seems that the layout would extend along the North axis, until about 372 m (from the tower), whereas towards the South it be prolonged until around 332 m. This is due to the calculation of the constant blocking factor, which affects more the northern heliostats because of their inclination that leads to a larger radial distance between them. In addition, to the East and West axis, the field symmetric side could measure about 344m. With our model, the layout reaches 362 m along the North axis and 331 m towards the South axis, and lateral sides each measure 343 m.

2) Arrangement of the heliostats by zones: The present work provides us with a total number of 858heliostats, shared on three zones, the first region composed of 5 lines of 22 heliostats each, the second contains 7 lines of 44 heliostats each and the third includes 5 lines of 88 heliostats each (table I). It seems that the configuration Collado [5] model, in the first lines is denser, because the number of heliostats that can be counted on reaching the end of the second zone (line 12) is 519 heliostats, which can be compared to 418 heliostats of the present work, due to the pure radial staggered configuration (the number of heliostats is doubled from one line to the next zone line). However, the two schemes have very similar values for longer distances between heliostats and tower base (Y = 372 m, Collado[5] model, Y = 362 m present work).

3) Efficiency of the field: We can see that the red area located north of the tower is the most efficient and green area located south of the tower is the least efficient . By comparing

TABLE I.   VARIATION IN THE NUMBER OF HELIOSTATS WITH THE NUMBER OF LINES

Line number	1	2	3	4	5	6	7	8	9	10	11	12	13	14	15	16	17
Collado model	22	22	22	39	39	39	39	39	39	73	73	73	73	73	73	73	73
Present work	22	22	22	22	22	44	44	44	44	44	44	44	88	88	88	88	88

the results of the two models we have in figure 2; (Model Collado): 884 heliostats and an average efficiency of 75.77% , in the figure 3 (our work) 858 heliostats and an average efficiency of 76. 15%. The results obtained by our model for a preliminary design of a field of heliostats are in good agreement with those obtained by Collado[5], and that as for the geometric distribution of the solar field, as the values of the efficiency optics.
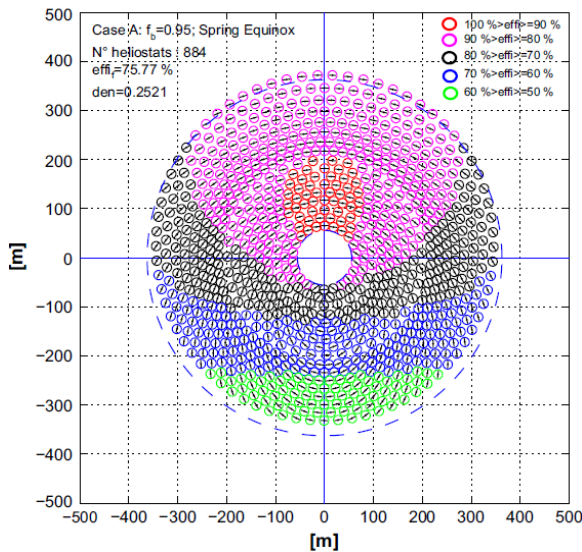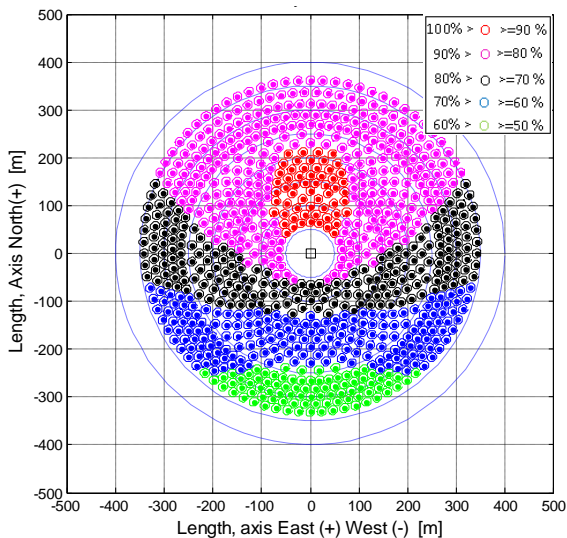

Fig. 2. Distribution of optical efficiency [5]

Fig 3. Distribution of optical efficiency (our work)

B. Flux distribution on the receiver

For the flux distribution on the receiver we compare our results with those of Collado 2010[15]. We present in the table II, the coordinates of heliostats tested and their distance D to the aim point [15].

TABLE II.   HELIOSTATS POSITIONS [15]

#	name	X(m)	Y(m)	Z(m)	D(m)
1	C1	-64.02	150.26	6.06	165.23
2	H62	-48.91	82.30	4.79	99.83
3	H14	9.75	41.15	4.27	51.8

1)   Central profiles: In figures 4,5 and 6, the blue curves represent the centrale profile (i.e, yr = 0) of the flux density following the model of Colado[15], in red the measured profile [15] and in green our simplified work. As can be observed the coincidence of the shape of the curves is remarkable, which suits very well. For the heliostat # 1 (Fig. 4) , we can notice according to the curves, when the flux density takes the value 6.18 kw/m^2 , then x_r have the values (x_r =-0.785 m) for the blue curve and (x_r=-0.7830 m) for the green curve , the difference between the two points reach the value $\Delta x_{r1} = -0.0015$m for a relative error of 0.19%. For the heliostat # 2 (Fig.5), the flux density takes the value of 8.52 kw/m^2 with (x_r=-0.6854 m) for the blue curve and (x_r=-0.7040 m) for the green curve , such as   the difference $\Delta x_{r2} = -0.0186$m between the two points of position for a relative error of 2.71 % . For the heliostat # 3 (Fig. 6) the flux density takes the value 8.88 kw/m^2 with (x_r=-0.6200 m) for the blue curve and (x_r=-0.6125 m) for the green curve , such as the difference $\Delta x_{r3} = -0.0075$m, for a relative error of 1.2%. A systematic comparaison of peak fluxes for Collado model [15], measured[15] and our work for this three heliostats located in different part of the field is presented In table III. We can notice that the difference in the peak fluxes take the high value 11.41 %, for the heliostat # 3 which is the nearest from the tower. This is due to the errors of the simplifying hypotheses which become important when the distance between the center of the receiver and the center of each heliostat decreases, that affect the result of calculating the density of flux which will give a detachment of our curve to that of Collado [15] . We think this approach is quick, easy and can be useful for studying the behavior of the solar flux on the receiver in a preliminary way.
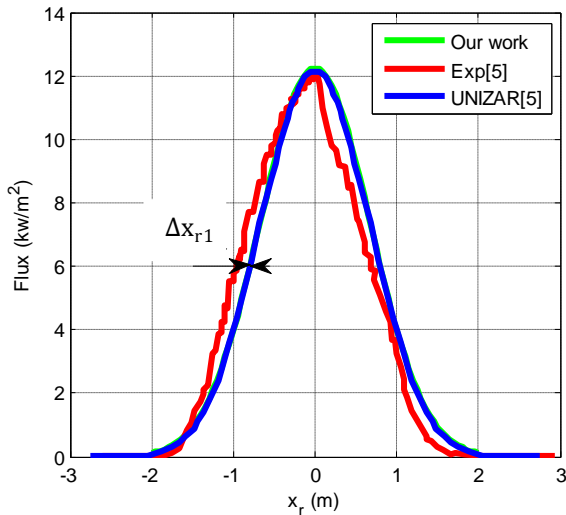
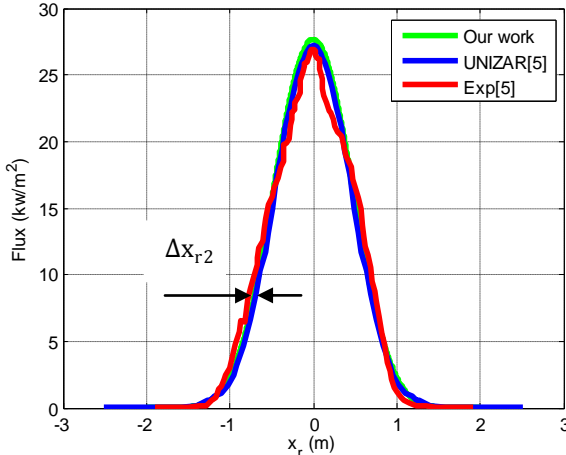Fig. 4 Measured and calculated central profiles for heliostat #1

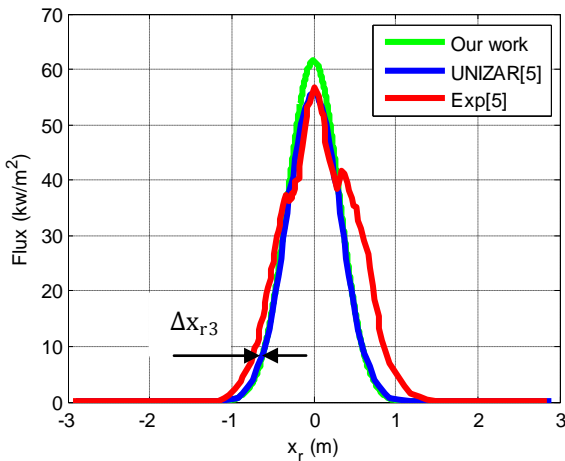Fig. 5 Measured and calculated central profiles for heliostat #2

Fig. 6 Measured and calculated central profiles for heliostat #3

TABLE III. COMPARATIVE OF PEAK FLUXES OF UNIZAR[15], MEASURED[15] AND OUR WORK

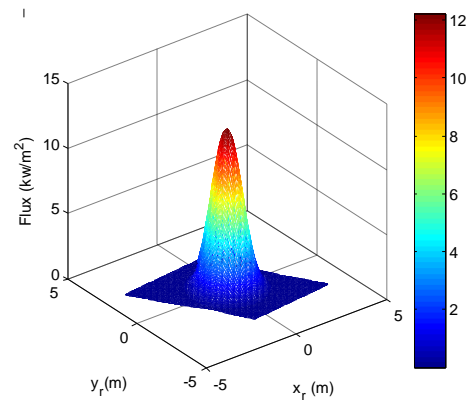| Heliostat number	#1	#2	#3
Peak flux Exp[15] (W/m^2)	12.1086	26.9194	56.7647
Peak flux Unizar [15] (W/m^2)	12.1380	27.2004	55.8235
Peak flux Our work (W/m^2)	12.2654	27.8346	62.1927
Difference (%) Exp[15]/ Our work	1.2949	3.3998	9.5623
Difference (%) Unizar [15]/ Our work	1.05	2.33	11.41

Fig.7 flux density in three dimensions on the receiver plane for heliostat #1

3) Contours of the total flux density for 3 heliostats: In the figure 8 we have a representation of the superposition of the contours of the flux density for 3 heliostats. The sunspot can be visualized by a series of curves (iso-density) concentric circular in shape. Their values were decreasing by moving away from the center of the receiver.
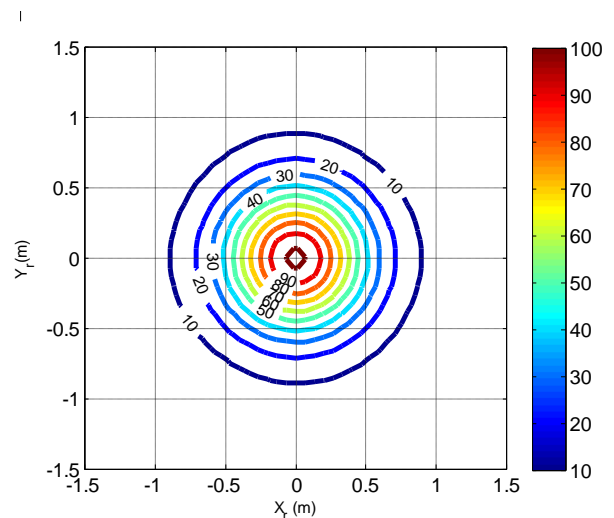

Fig.8 Contours of the total flux density for 3 heliostats

2) Flux density in three dimensions: Figure 7 presents the three-dimensional flux density for heliostat #1. This is a gaussian curve, the three heliostas examined have the same shape, and that what it can found in the literature concerning reflection on a fixed point[16]

V.   CONCLUSION

In the present work an optimization based on the full radial staggered configuration of surrounding field of heliostats has been presented. The results of our model are in good agreement with those obtained by Collado , both in the geometric distribution of the solar field, as the values of the optical efficiency, which has allowed us to continue the work for studying and comparing the solar flux distribution on vertical receiver reflected by each heliostat. The accuracy of the flux distribution has been checked for a range of distances to the tower. The superposition of flux density contours of overall sunspot for three heliostats has been presented. This work on vertical receptor plan allows a generalization of a cylindrical surface, with some modifications that should be made on the form of the receiving surface

REFERENCES

[1] Nikola Lorenz, Alberto Abanades, "A review on the application of liquid metals as heat transfer fluid in concentrated solar power technologies", International journal of hydrogen energy, vol. 41,(2016), pp 6990-6995.

[2] Abdullah A. Alzahrani, Ibrahim Dincer, " Design and analysis of a solar tower based integrated system using high temperature electrolyzer for hydrogen production", Int. J. Hydrogen Energy, vol. 41, (2016),pp 8042-8056

[3] M. B. K. Lodhi, " Collection and storage of solar energy", Int. J. Hydrogen Energy, Vol. 14, N°. 6,(1989), pp 379-411.

[4] Siala, F.M.F., Elayeb, M.E., '' Mathematical formulation of a graphical method for a no-blocking heliostat field layout '', Renewable Energy 23 (2001), pp77–92.

[5] Collado, F.J., '' Preliminary design of surrounding heliostat fields'', Renewable Energy 34 (2009) 1359–1363.

[6] Collado, F.J., Turégano, J.A., ''Calculation of the annual thermal energy supplied by a defined heliostat field'', Solar Energy 1989;42:149-65

[7] Francisco J. C., Jesús, G., '' Campo: Generation of regular heliostat fields '', Renewable Energy, Volume 46, (October 2012), Pages 49-59.

[8] E.Bilgen and C. Bilgen, " Hydrogen as a vector for central receiver solar utilities", Int. J. Hydrogen Energy, vol. 7,N°. 12, (1982), pp. 977-984

[9] Atif, M, Al-Sulaiman. F.A, "development of a mathematical model for optimizing a heliostat field layout using differential evolution method", Int. J.Energy Res.(2015), vol. 39, pp.1241-1255.

[10] Ballestrin, B., Marzo, A., ''Solar radiation attenuation in solar tower plants '', Solar energy, Vol. 86, (2012), pp.388-392.

[11] Chong, K.K., Tan, M.H., ''Comparison study of two different sun-tracking methods in optical efficiency of heliostat field '', International Journal of Photo energy, (2012), Article ID 908364, 10 pages.

[12] P. Garcia, A. Ferriere, and J.-J. Bezian, ―Codes for solar flux calculation dedicated to central receiver system applications: a comparative review _', Solar Energy, vol.82, no. 3,(2008), pp. 189-197.

[13] A. Sanchez-Gonzalez, D. Santana, " Solar flux distribution on central receivers : A projection method from'', Renewable Energy. vol. 74, (2015), pp. 576-587.

[14] Collado, F.J., Gomez, A., Tureganot, J.A., '' An analytic function for the flux density due to sunlight reflected from a heliostat '', Solar Energy, Vol. 37, N°.3, (1986), pp.215-234.

[15] Collado, F.J., '' One-point fitting of the flux density produced by a heliostat '', Solar Energy, Vol.84, (2010), pp. 673-684.

[16] Biggs .F, vittitoe.C. N, " the helios model for the optical behavior of reflecting solar concentrators", SAND76-0347, alburquerque (1979)